Journal Pre-proof

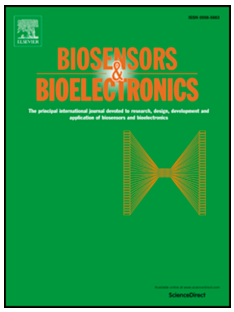

# 3D DNA nanosphere-based photoelectrochemical biosensor combined with multiple enzyme-free amplification for ultrasensitive detection of cancer biomarkers

Xiaoshan Gao, Shuyan Niu, Junjun Ge, Qingyu Luan, Guifen Jie

PII: S0956-5663(19)30857-7

DOI: https://doi.org/10.1016/j.bios.2019.111778

Reference: BIOS 111778

To appear in: *Biosensors and Bioelectronics*

Received Date: 28 July 2019

Revised Date: 8 October 2019

Accepted Date: 9 October 2019

Please cite this article as: Gao, X., Niu, S., Ge, J., Luan, Q., Jie, G., 3D DNA nanosphere-based photoelectrochemical biosensor combined with multiple enzyme-free amplification for ultrasensitive detection of cancer biomarkers, *Biosensors and Bioelectronics* (2019), doi: https://doi.org/10.1016/j.bios.2019.111778.

This is a PDF file of an article that has undergone enhancements after acceptance, such as the addition of a cover page and metadata, and formatting for readability, but it is not yet the definitive version of record. This version will undergo additional copyediting, typesetting and review before it is published in its final form, but we are providing this version to give early visibility of the article. Please note that, during the production process, errors may be discovered which could affect the content, and all legal disclaimers that apply to the journal pertain.

© 2019 Published by Elsevier B.V.

Journal Pre-proof

# 3D DNA nanosphere-based photoelectrochemical biosensor combined with multiple enzyme-free amplification for ultrasensitive detection of cancer biomarkers

Xiaoshan Gao[a], Shuyan Niu[a], Junjun Ge[a], Qingyu Luan[b], Guifen Jie[a*]

a Key Laboratory of Optic-electric Sensing and Analytical Chemistry for Life Science, MOE; Shandong Key Laboratory of Biochemical Analysis; Key Laboratory of Analytical Chemistry for Life Science in Universities of Shandong; College of Chemistry and Molecular Engineering. Qingdao University of Science and Technology, Qingdao 266042, PR China.

b Yucheng Vocational education school, Yucheng, Shandong Province，251200, China

**A B S T R A C T**

In this work, a new 3D DNA nanosphere was ingeniously designed and fabricated, which was used to combine with multiple enzyme-free amplification strategy to develop a photoelectrochemical (PEC) biosensing platform for ultrasensitive detection of carcinoembryonic antigen (CEA). The 3D DNA nanostructure was self-assembled by base complementary pairing in a few minutes and rolling circle amplification (RCA) reaction. The intense photocurrent derived from Au NPs/ZnSe QDs can be effectively decreased by 3D DNA nanospheres assembled on the electrode, making photoelectric signal present “off” state. The specific binding of target CEA with its hairpin (HP1) aptamer opens HP1 structure, which initiated multiple enzyme-free strand displacement amplification (SDA) reaction and generated a large number of single strands DNA S1. Then S1 competitively binds to capture DNA on the electrode to release 3D DNA nanospheres, thus the photocurrent signal became “on” state for achieving amplified assay of target CEA. The proposed PEC biosensor exhibits excellent performance with a wide linear range of 1.0 fg/mL to 10 ng/mL and a low detection limit of 0.12 fg/mL for CEA, which was successfully applied for the assay of real serum samples with good precision. The reported strategy opens a new simple way for PEC biosensor using DNA nanostructure, showing huge potential in clinical application research.

*Keywords***:** 3D DNA nanosphere ZnSe quantum dot recycling amplification PEC

*Corresponding author.

*E-mail address: guifenjie@126.com.

Journal Pre-proof

## 1. Introduction

Carcinoembryonic antigen (CEA) is an important cancer biomarker, early diagnosis of cancer by biomarkers plays a vital role for cancer treatment (Zimmer and Thomas., 2001). Many clinical data showed that the CEA level is increased in the serum of breast cancer and other tumors (Hine, et al., 1978). Therefore, ultra-sensitive detection of CEA is significantly important in clinical diagnosis.

In the past few years, with increasing demand for bioanalysis, more advanced biotechnologies have been studied (Ge, et al., 2019; Chen, et al., 2012a; Mayer and Hafner., 2011; Ronkainen, et al., 2010). Significantly, PEC biosensing has been developed rapidly in bioanalysis (Li, et al., 2019a; Li, et al., 2014). Unlike optical technology (Kumar, et al., 2015; Xie, et al., 2013; Yuan, et al., 2014), PEC instruments are simple and compact, and the PEC detection methods displayed lower background signal and higher sensitivity due to separation of light source and photocurrent (Liu, et al., 2016; Long, et al., 2011; Zhu, et al., 2016). PEC sensors have superior performance and are able to identify target in mixed samples compared to other detection methods (Shu, et al., 2016), so significant progress has been made in the field of PEC bioassays, such as disease diagnosis (Dai, et al., 2016), food safety (Zhang, et al., 2017) and medicine research (Zheng, et al., 2017). However, photoactive materials are important for performance of PEC sensors (Kwon, et al., 2014; Josset, et al., 2008). In the past, metal oxides have been intensively studied as photoactive materials (Luo, et al., 2012; Gogurla, et al., 2014). Quantum dots (QD) containing cadmium and plumbum are toxic and has low photoelectric conversion efficiency, limiting their application in bioanalytical directions (Nishi, et al., 2013; Zang, et al., 2014; Wang, et al., 2009). ZnSe QDs are excellent photoactive substances because of their low toxicity, good photostability, good water solubility and biocompatibility (Chen, et al., 2012b), which exhibited great potential application in bioanalysis.

DNA is considered to be one of the most promising materials for biosensors and has unprecedented promise in nanotechnology (Roh, et al., 2011). In recent years, DNA nanostructures have attracted much attention due to their excellent programming performance, controllability and high precision, which have been widely used in the field for biological analysis (Meng, et al., 2016; Hariri, et al., 2015; Li, et al., 2019b).

To improve the detection sensitivity of bioassays, some signal amplification strategies have

Journal Pre-proof

been introduced for bioassay, such as strand displacement amplification (SDA) (Wang, et al., 2017), rolling circle amplification (RCA) (Zeng, et al., 2013), and exponential isothermal amplification reaction (EXPAR) (Zhao, et al., 2018). Common rolling ring amplification products are nanowires, which were used to mark the signal molecules (Zhang, et al., 2018a), trigger exponential amplification of targets (Li, et al., 2018) and capture more targets (Zheng, et al., 2016). Most amplification processes were carried out with the aid of enzyme, which suffer from instability or high background signal (Xie, et al., 2017). Notably, enzyme-free target recycling amplification with double-output design strategy have aroused wide interest in bioassay due to their excellent amplification efficiency and high selectivity, in which one target can induce to output a large amount of DNA mimic targets (Li, et al., 2017; Huo, et al., 2017).

In this study, we fabricated a novel 3D DNA nanosphere with unique steric structure by rolling ring amplification reaction for the first time, and used it to skillfully design a new kind of PEC biosensor by coupling with enzyme-free amplification strategy for sensitive assay of CEA. In particular, the target-induced enzyme-free SDA reaction is rapid and displayed high amplification efficiency, and the large DNA nanosphere is simple and can lead sensitive PEC signal change, thus this study opened a new avenue for developing promising PEC biosensor based on DNA nanostructures. Scheme 1 showed the principle for the PEC biosensor. Firstly, target CEA was introduced to open the hairpin structure (HP1, blue portion is CEA aptamer). The exposed red part of HP1 competes to bind with S0 on magnetic beads (MB) to release S1. Subsequently, S2 further replaced the red part of HP1 and another S1 by competitive binding with S0, the released HP1 continues to interact with S0 to achieve recycling amplification, finally generating large amounts of S1. At the same time, the 3D DNA nanosphere is assembled by base pairing of single-stranded DNA (Zhang, et al., 2018b) and RCA reaction. The photocurrent signal from ZnSe QDs/Au NPs was obviously decreased by the 3D DNA nanospheres immobilized on the electrode due to increased steric hindrance, resulting in PEC “signal off” response. After target CEA-induced S1 competes to hybridize with the capture probe DNA on the electrode, 3D DNA nanosphere is removed from the electrode, generating “signal on” state. The enhanced photocurrent signal is proportional to the concentration of CEA, achieving ultrasensitive detection of CEA at low concentration. Therefore, the proposed PEC biosensor has great potential for early clinical diagnosis.

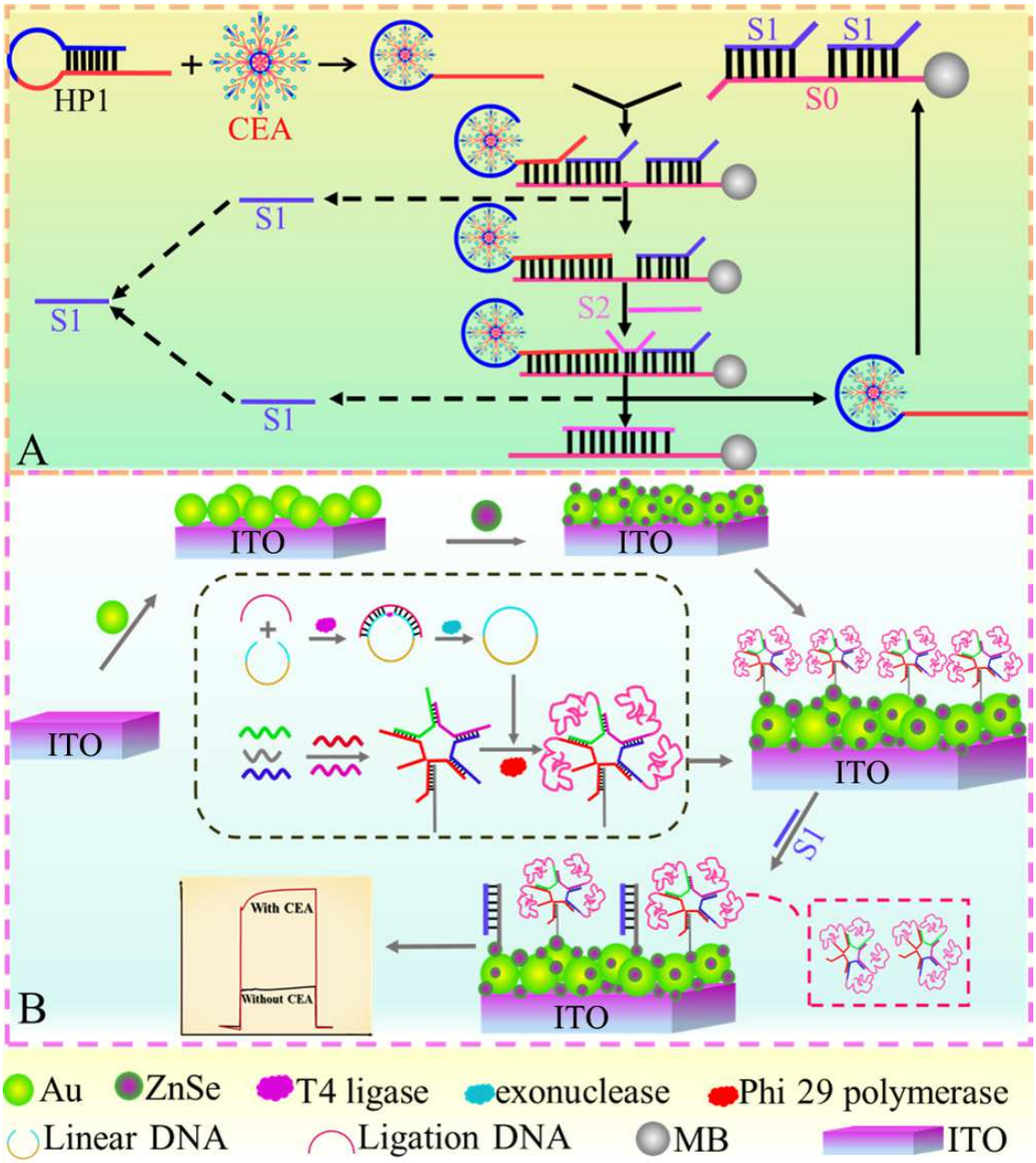


**Scheme 1.** Schematic diagram of this proposed PEC biosensor for CEA determination. (A) Enzyme-free target cycling amplification strategy for generating S1; (B) Fabrication of the PEC "signal-off-on" biosensor based on ZnSe QDs/Au NPs and 3D DNA nanospheres.

## 2. Experimental section

### *2.1. Synthesis of ZnSe QDs*

The water-soluble ZnSe QDs were prepared by two steps. NaHSe solution was prepared according to the method (Gu, et al., 2008). In brief, 0.22 g Se powder (0.003 mol) and 0.2645 g $NaBH_4$ (reducing agent) were mixed in 8 mL deionized water and heated at 50 $^{\circ}C$ with $N_2$ bubbling for 5-6 minutes to obtain a clear NaHSe solution. Subsequently, 0.4587 g $Zn(CH_3COOH)_2$ and 750 μL mercaptopropionic acid (MPA, which is used to functionalize ZnSe

Journal Pre-proof

QDs with carboxyl groups) were mixed in 50 mL deionized water, and the pH was adjusted to 9-10 by NaOH. Then, 5.7 mL of the freshly prepared NaHSe solution was injected into the $N_2$-saturated $Zn(CH_3COOH)_2$/MPA solution. The mixture was refluxed in a boiling water bath for 5 hours. The as-prepared ZnSe QDs were cooled to room temperature (RT) and cleaned three times by precipitation with excess isopropanol alcohol. Finally, ZnSe QDs were dispersed in deionized water.

*2.2. Synthesis of Au NPs*

Gold nanoparticles (Au NPs) were prepared according to the reported method (Frens., 1973). In brief, all glassware was cleaned in aqua regia ($HCl/HNO_3$=3:1), rinsed with $H_2O$, and then oven-dried prior to use. 500 µL of 1.0% $HAuCl_4$ solution (as a source of Au) was added to 50 mL of boiling water and refluxed for 10 s, then 0.5 mL of sodium citrate (1.0 wt%, as a reducing agent) was injected into the above solution with vigorous stirring to reduce $HAuCl_4$ to Au NPs. After boiling for a while, the solution turned brilliant ruby red, and the heating was stopped. The stirring was continued for an additional 30 min, then the solution was cooled to room temperature for further use. The whole process is dark.

*2.3. Preparation of the sample solution*

First of all, the DNA sequences were pretreated, 20 µL of hairpin probe 1 (HP1, 1 µM) was treated by heating DNA sequences to 95 °C for 5 min and cooling to room temperature naturally. 20 µL of S0 (1 µM), 45 µL of S1 (1 µM) were mixed together and treated by annealing to obtain doubled-stranded DNA (dsDNA). 100 µL of carboxyl-modified magnetic beads (MB) were washed three times with 200 µL of PBS (pH 7.4, 0.1 M $Na_2HPO_4 \cdot 12H_2O$, 0.1 M $NaH_2PO_4 \cdot 2H_2O$, 0.1 M KCl), and activated with 200 µL of 0.1 M PBS containing 10 mg NHS and 20 mg EDC for 40 min with gentle shaking at room temperature, then the supernatant was discarded. The above dsDNA was added to the activated magnetic bead solution with gentle shaking for 12 h, and 65 µL of dsDNA-MB solution was obtained by magnetic separation, then the supernatant was discarded. 20 µL of HP1 (1 µM), 20 µL of S2 (1 µM), and different concentrations of CEA were added into the centrifuge tube and kept shaking at room temperature for 2 h. Next, the supernatant (referred to as sample solution) was collected by magnetic separation.

*2.4. Preparation of circle DNA template*

The circle DNA template was prepared according to the reported method (Ren, et al., 2016). 2.5

Journal Pre-proof

μL of phosphorylated linear DNA (100 μM), 5 μL of ligation DNA (100 μM), 5 μL of ultrapure water and 1.5 μL of 10×T4 buffer were mixed and annealed at 95 °C for 5 min, and then slowly cooled to room temperature. 1 μL of T4 DNA ligase (400 U $\mu L^{-1}$) was added to the mixture and incubated at 20 °C for 10 hours. After the T4 DNA ligase was inactivated at 65 °C for 10 min, 2.5 μL of 10×exonuclease I buffer, 2.5 μL of 10×exonuclease III buffer, 2 μL of exonuclease I (20 U $\mu L^{-1}$) and 2 μL of exonuclease III (100 U $\mu L^{-1}$) were added to the above mixture to incubate at 37 °C for 2 h for forming circular DNA template. The mixture was finally heated at 80 °C for 15 min to denature the exonuclease I and exonuclease III.

*2.5. Preparation of the 3D DNA nanosphere*

Probe1 (2.5 μL, 10 μM), probe2 (2.5 μL, 10 μM), A1(2.5 μL, 10 μM), A2 (2.5 μL, 10 μM) and capture probe (1 μL, 10 μM) were added to a 1.5 mL centrifuge tube and sealed with a parafilm, then the above centrifuge tube was heated to 95 °C and left on ice immediately, and the well-designed 3D DNA nanosphere precursor was synthesized. Next, to initiate the RCA reaction on the basis of 3D DNA nanosphere precursor, 11 μL of 3D DNA nanosphere precursor solution, 2.5 μL of 10× reaction buffer, 2.5 μL of phi29 DNApolymerase (10000 U $mL^{-1}$), 10 μL of dNTPs (10 mM), 7.5 μL of circle DNA template, and 15 μL of ultrapure water were added to a 1.5 mL centrifuge tube quickly to incubate for 1.5 h at 37 °C, and the well-designed 3D DNA nanosphere was synthesized.

*2.6. Fabrication of the photoelectrochemical (PEC) biosensor for CEA detection*

A piece of bulked indium tin oxide (ITO) glass (sheet resistance≤6 Ω/square, 1 cm × 5 cm) was incised to small pieces of rectangular ITO, and then the nonconductive rubberized fabric with hollow-carved geometrical area of 0.25 $cm^2$ (0.5 cm × 0.5 cm) was pasted on the small piece of rectangular ITO glass to obtain the modified electrode. ITO glass was sequentially sonicated for 10 min in dilute hydrochloric acid solution, ethanol, and distilled water, respectively and dried with nitrogen. The fabrication process was schematically exhibited in Scheme 1B, after Au NPs solution (10 μL) was dropped on the surface of bare ITO electrode and dried naturally, the ZnSe QDs solution (10 μL) was dropped onto the electrode surface to form ITO/Au NPs/ZnSe QDs. Then the modified electrode was activated in PBS containing 10 mg of NHS and 20 mg of EDC for 30 min. After rinsing, 10 μL of amino-modified 3D DNA nanosphere was placed on the surface of Au NPs/ZnSe QDs modified electrode for 6 h in humid environment, and washed with

Journal Pre-proof

TE buffer to remove unlinked 3D DNA nanosphere. Subsequently, the modified electrode was incubated with 10 μL of the prepared sample solution at 37 °C for 2 h in humid environment, then it was rinsed to obtain the PEC biosensor.

The photocurrent measurements were carried out in PBS buffer (pH 7.4, 0.1 M) containing 0.1 mM AA by using ITO as the working electrode, a Pt wire counter electrode, and a saturated calomel electrode (SCE) as the reference electrode. The blue light was utilized as excitation light source and was turned on and off every 20 s (output power: >20 mW/cm$^2$, spectral range: 420–470 nm, peak wavelength: 465 nm).

## 3. Results and discussion

### *3.1. Topography and spectral characterization of the synthesized ZnSe QDs*

Figure 1A showed transmission electron micrograph (TEM) image of the synthesized ZnSe QDs, which exhibited uniform morphology with an average size of 3.5 nm in diameter. Moreover, the lattice fringe of 0.33 nm could be assigned to the (111) plane of ZnSe (Figure 1A, top inset). Figure 1B displayed the X-ray powder diffraction (XRD) pattern of ZnSe QDs, the diffraction peaks of the powder perfectly match the ZnSe standard card (JCPDS 37-1463). The three characteristic peaks appearing at 27.22°, 45.20°, and 56.15° corresponded to three lattice planes (111), (220) and (222) of ZnSe QDs (black), respectively. The sharp diffraction peaks demonstrated that the products have high purity and good crystal.

Figure 1C showed the UV-vis absorption and fluorescence (FL) spectra of ZnSe QDs and Au NPs. ZnSe QDs displayed a broad absorption peak at 465 nm (curve a) and a strong FL emission peak at about 470 nm (curve b, excitation wavelength: 203 nm). Curve c showed the UV-vis absorption spectrum of Au NPs, an absorption peak at 526 nm indicated the characteristic property of Au NPs. Figure 1D is the ECL-potential curve of ZnSe QDs, a strong ECL peak at -2.0 V was observed, the results demonstrated that ZnSe QDs have good optic-electric property.

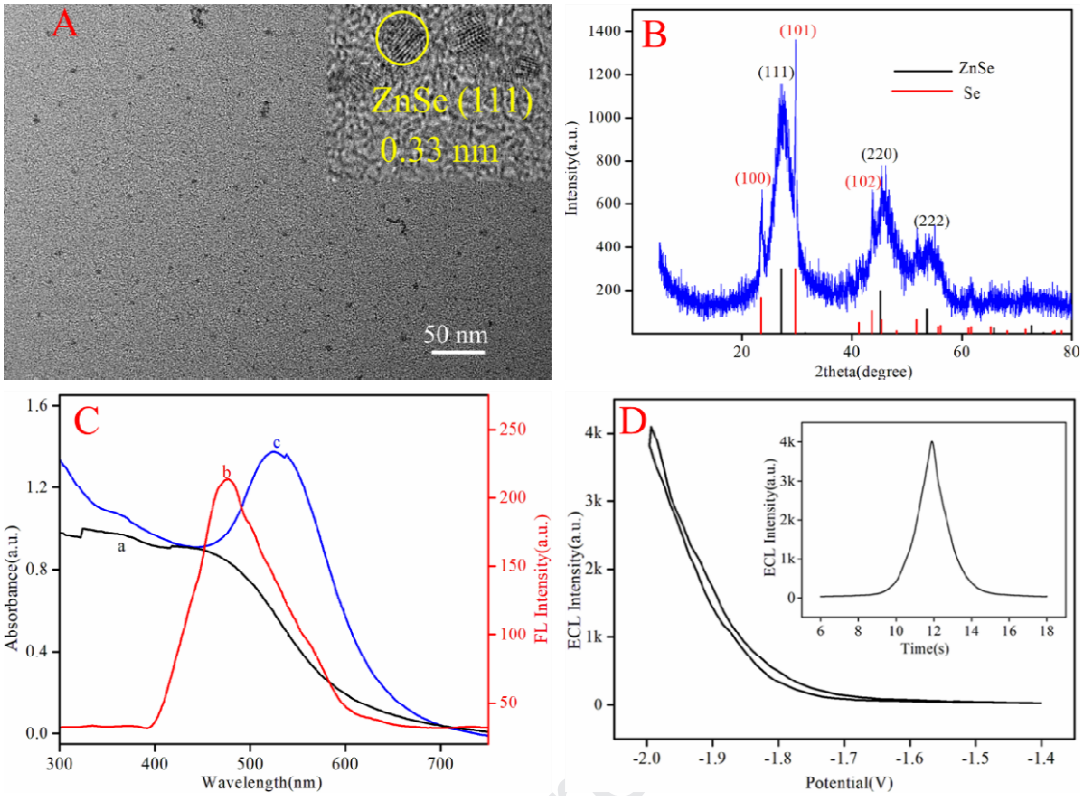


**Figure 1.** (A) TEM image (inset: HRTEM image) of ZnSe QDs; (B) XRD spectra of ZnSe QDs; (C) UV-vis absorption spectra of ZnSe QDs (a) and Au NPs (c), and fluorescence spectrum of ZnSe QDs (b); (D) ECL-potential curve (inset: ECL-time profile) of ZnSe QDs.

*3.2. ZnSe QDs photocurrent response and mechanism*

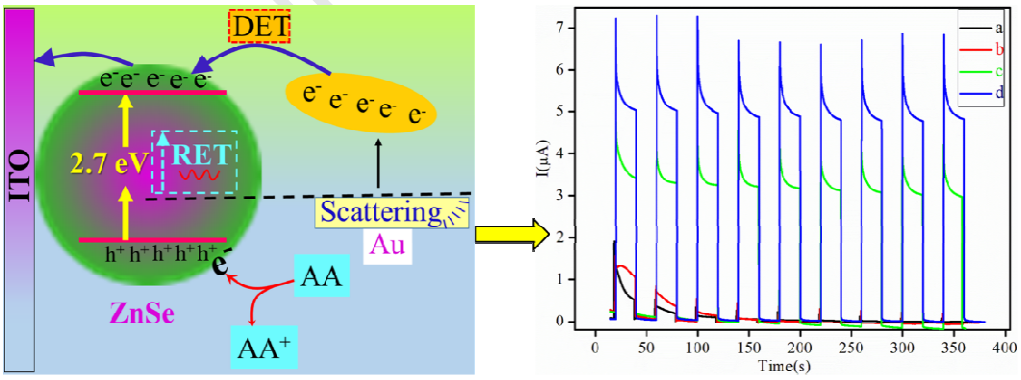


**Scheme 2.** PEC reaction mechanism, and photocurrent responses of ZnSe QDs in PBS (a) without AA and Au NPs, (b) with Au NPs, (c) with AA, (d) with AA and Au NPs.

The sensitivity of PEC bioassay depended on the photocurrent signal, which is related to the PEC reaction mechanism. The absorption and fluorescence emission spectra of ZnSe QDs are in blue light range, so the photocurrent was detected by blue light (Scheme 2). The photocurrent of ZnSe QDs is about 0.5 μA in PBS (curve a), whereas a nearly 7-fold increase of photocurrent was

Journal Pre-proof

obtained after adding ascorbic acid (AA) to PBS (3.5 μA, curve c). AA as electron donor can consume the photogenerated holes in the valence band (VB) of ZnSe QDs, which reduced the recombination rate of electron-hole pairs. When Au NPs were modified on the electrode, the photocurrent signal was further increased (curve d) and steady. The possible mechanism was shown in Scheme 2. The localized surface plasmon resonance (LSPR) effect of Au NPs could increase the light scattering, which improved the photoelectric conversion efficiency of ZnSe QDs, such electron transfer can attribute to the Fermi level rearrangement (Lee and Lo., 2009). Hot electrons from Au NPs to the conduction band (CB) of ZnSe QDs further injected to the electrode, triggering successive generation of photocurrent.

*3.3. Characterization of the 3D DNA nanosphere*

The assembled 3D DNA nanospheres were characterized by polyacrylamide gel electrophoresis (PAGE), transmission electron microscopy (TEM) and atomic force microscopy (AFM) (Figure 2). The distinct bands observed in lane1, lane2, lane3, lane4 and lane5 represent the single-stranded DNA of Probe1, Probe2, A1, A2 and Capture Probe (Figure 2A). By rapid annealing reaction of the five DNA strands, a band with very low mobility was observed in lane 6, illustrating the successful self-assembly of the precursor of 3D DNA nanosphere. On the basis of the precursor, rolling circle amplification (RCA) was carried out to obtain 3D DNA nanosphere. Due to the relatively large molecular mass of 3D DNA nanosphere, a single and bright band appeared at the top in lane 7, indicating that the 3D DNA nanosphere was successfully formed.

Moreover, the morphology and size of 3D DNA nanosphere were characterized by TEM (Figure 2B) and AFM (Figure 2C) images, the results showed that a lot of uniform globular structure were observed, and the average diameter was 35 nm ±10 nm. Figure 2D showed that the measured height of the 3D DNA nanosphere was 5.8-6.5 nm. The TEM and AFM prove that the 3D DNA nanosphere was successfully formed.

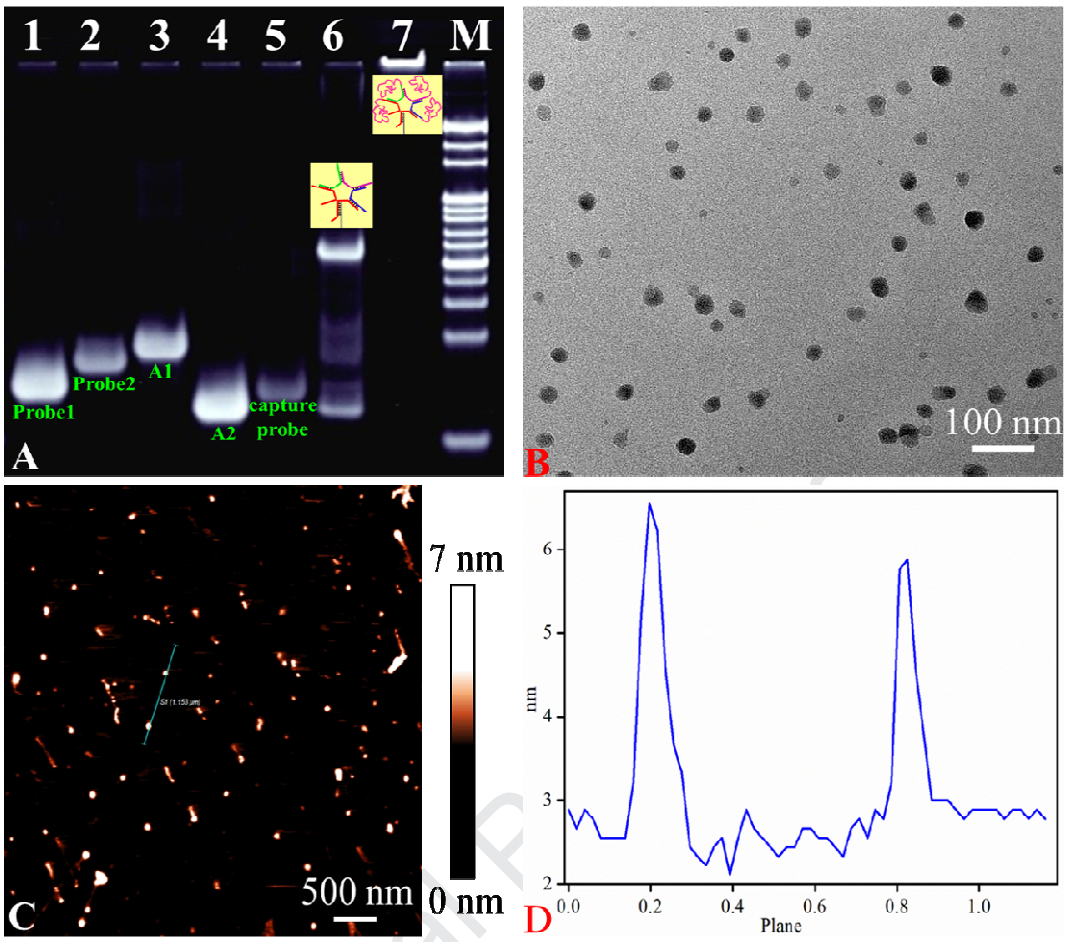


**Figure 2.** (A) PAGE characterization of the 3D DNA nanosphere. Lane 1: Probe1 (2 μM); lane 2: Probe 2 (2 μM); lane 3: A1 (2 μM); lane 4: A2 (2 μM); lane 5: Capture Probe: (2 μM); lane 6: 3D DNA; lane 7: 3D DNA nanosphere; lane M: marker. (B) TEM image of the 3D DNA nanosphere. (C) AFM image of 3D DNA nanosphere. (D) Cross-sectional profile of the deep blue lines in panel C.

*3.4. Electrochemical characterization of the PEC biosensor*

To investigate the modification process of the PEC biosensor, the photocurrent signals of the modified electrodes are shown in Figure 3A. When Au NPs were assembled on the electrode, the photocurrent was slightly higher (curve b) than the bare electrode (curve a), which was attributed to the excellent conductivity of Au NPs. Then, the highest photocurrent signal was obtained after modification of ZnSe QDs (curve c), demonstrating that ZnSe QDs possess good PEC property. After the 3D DNA nanospheres were assembled on the electrode, the large DNA structure has greater steric hindrance effect, and the negatively charged phosphate skeletons increased repulsion, which blocks the transfer of AA to the electrode, so the photocurrent signal significantly decreased

(curve d). Subsequently, when target CEA-induced S1 was linked to the electrode, the photocurrent signal increased remarkably (curve e), as S1 competitively bind to the electrode to remove 3D DNA structure, suggesting that the PEC biosensor for CEA was successfully developed.

To further demonstrate the successful preparation of PEC biosensor, the assembly steps of the sensing interface were characterized by electrochemical impedance spectroscopy (EIS) (Figure 3B). In comparison to bare ITO (curve a), the Au NPs modified electrode exhibited a smaller charge-transfer resistance (Ret) (curve b), suggesting that Au NPs facilitated the electron transfer. Then the modified ZnSe QDs increased Ret value (curve c). The Ret increased significantly after the 3D DNA nanospheres were assembled on the electrode (curve d) due to increased negative charges of DNA and steric hindrance effect. However, the Ret obviously decreased after S1 single strands competitively linked to the electrode by replacing DNA nanospheres (curve e, CEA induced generation of S1). Based on the above results, we concluded that the PEC biosensor was successfully constructed and could be applied for CEA detection.

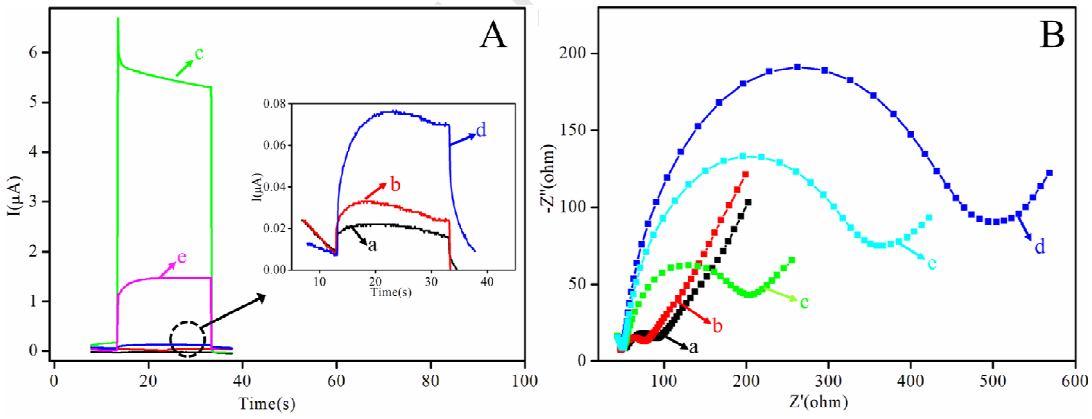


**Figure 3.** (A) Photocurrent responses, and (B) EIS of the PEC biosensor at different stages. (a) bare ITO, (b) ITO/Au NPs, (c) ITO/Au NPs/ZnSe, (d) ITO/Au NPs/ZnSe/3D DNA nanosphere, (e) ITO/Au NPs/ZnSe/3D DNA nanosphere in the presence of target CEA (1.0 ng/mL).

*3.5. SEM characterization of the biosensor*

The surface topography of the modified electrode at each step was monitored by scanning electron microscopy (SEM) images. As shown in Figure S1A, numerous large Au nanoparticles with a diameter of 50-70 nm were covered on the electrode. Figure S1B displayed large amounts of densely distributed small dots of ZnSe QDs on the electrode. In addition, the elemental mapping images demonstrated the existence of Zn, Se, and Au elements within the surface of

Journal Pre-proof

ITO/Au NPs/ZnSe QDs (Figure S1D). After 3D DNA nanospheres were further assembled on the electrode, a uniform layer of larger-sized nanospheres was formed on the electrode surface (Figure S1C). Thus the SEM characterization indicated the successful fabrication of the modified electrodes for PEC biosensing.

*3.6. Optimization of the experimental conditions*

The experimental conditions for PEC measurements were optimized, the concentration of capture probe, the time of RCA reaction, the volume of phi29 DNA polymerase and Au NPs were investigated. As the PEC sensing signal is related to the 3D DNA nanosphere structure, which is affected by the volume of phi29 DNA polymerase and the time of RCA reaction. As shown in Figure S2A, the photocurrent response exhibited a gradual decrease with increasing volume of phi29 DNA polymerase (10000 U $mL^{-1}$), and reached a minimum at 2.5 μL. Figure S2B displayed the photocurrent responses to different RCA reaction time, the responses decreased and reached the lowest value at 1.5 h. Therefore, we chose 2.5 μL of phi29 DNA polymerase and 1.5 h of RCA reaction time as the optimal conditions.

As displayed in Figure S2C, the photocurrent decreased gradually with increasing concentration of capture probe, and then reached a platform at 10 μM, suggesting that the 3D DNA nanospheres reached saturation and the concentration of capture probe was determined to be 10 μM.

The volume of Au NPs on the electrode was also optimized, the result was shown in Figure S2D. With the increase of Au NPs volume, the photocurrent signal increased gradually and reached a maximum at 20 mL, so 20 μL of Au NPs was used in the work. It should be noted that the Au NPs with an optimal volume can induce to generate the highest photocurrent, and can be further combined with the 3D DNA nanosphere with an optimal size can result in maximum change of photocurrent, which is favorable for sensitive assay of the biosensor.

*3.7. PEC analysis of the biosensor for CEA detection*

The photocurrent signal responses of the PEC biosensor to different concentrations of CEA were detected. In the blank solution without CEA, the PEC response of the biosensor was very low (Figure 4A, curve a). However, in the presence of CEA, the PEC response obviously increased due to less resistance of electron transfer, which proved that the CEA-converted DNA

S1 replaced the DNA nanospheres on the electrode. The results demonstrated that the PEC biosensor based on 3D DNA nanospheres is feasible for CEA detection.

Under optimal conditions, the performance of this PEC biosensor for CEA detection was investigated. As shown in Figure 4A, the PEC signal improved gradually with increasing concentrations of CEA from 1.0 fg/mL to 10 ng/mL (curves a-i), demonstrating that the concentration of CEA can be quantitatively detected by the PEC signal.

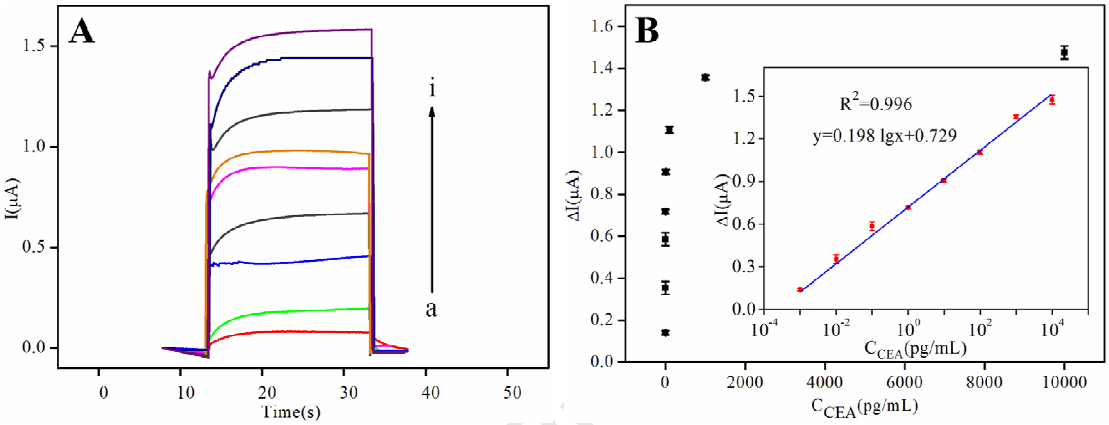


**Figure 4.** (A) PEC responses of the biosensor to various CEA concentrations: 0 ng/mL, 1.0 fg/mL, 10 fg/mL, 100 fg/mL, 1.0 pg/mL, 10 pg/mL, 100 pg/mL, 1.0 ng/mL, and 10 ng/mL (from a to i). (B) Relationship between ΔI (deducting background, $\Delta I = I - I_0$) and CEA concentration (inset: calibration plot for CEA detection), error bars represent standard deviations of three parallel experiments.

A good linear relationship between the PEC response changes and CEA concentrations was obtained (Figure 4B), and the linear regression equation for CEA was $y = 0.198 \lg x + 0.729$ ($R^2$ = 0.996), where y, x, and $R^2$ represented ΔI ($\Delta I = I\text{-}I_0$, $I_0$ was the current response of the black solution; I was the current response of CEA at different concentrations), CEA concentration and correlation coefficient, respectively. The linear range was 1.0 fg/mL to 10 ng/mL, and the detection limit was $1.2 \times 10^{-4}$ pg/mL (calculated from the expression of 3σ/N, σ is the standard deviation of the blank and N is the slope of the corresponding calibration curve). Furthermore, the analytical performance (including linear range and detection limit) of the proposed PEC biosensor for CEA was better than those of previously reported methods (Table S2), these results demonstrate the proposed PEC biosensor with wider linear range and lower detection limit is promising for clinical CEA detection.

Journal Pre-proof

*3.8. Selectivity, stability and reproducibility of this PEC biosensor*

The selectivity of this method was investigated by assaying the interfering substance, such as alpha-fetoprotein (AFP), thrombin (TB), estradiol (E2), luteotropic hormone (LH), human IgG, and their mixture with the target. An obviously higher PEC signal change can be found for the target CEA and the mixture sample compared with responses of AFP, TB, E2, LH, IgG at the same concentration and the blank (Figure S3A), indicating that the PEC biosensor displayed an excellent selectivity for CEA determination due to the high affinity and specificity of CEA with its aptamer HP1.

Long-term stability of the proposed biosensor was evaluated by continuously testing the PEC signal response of the biosensor to 1.0 ng/mL CEA under optimal experimental conditions (Figure S4). The prepared biosensor was stored in PBS buffer solution at 4 °C and measured every 3 days under the same conditions. The PEC signal of the biosensor did not exhibit any noticeable undulation in the presence of 1.0 ng/mL CEA within 13 days, and the signal response at the 13st day was 95.2% of that in the initial one. The results suggested that the proposed biosensor showed good stability.

To investigate the reproducibility of the PEC biosensor for detecting CEA, a series of five duplicate measurements of 1.0 ng/mL CEA were used for estimating the precision, and the relative standard deviation (RSD) was 4.3%, suggesting that the proposed biosensor has good reproducibility.

*3.9. Application of the PEC Biosensor for CEA detection in human serum samples*

The practical applications of the designed PEC biosensor were investigated, three kinds of human serum samples including breast cancer serum samples, liver cancer and normal human serum samples obtained from the hospital were utilized to test the application feasibility of the biosensor. The CEA levels were calculated according to the equation in Figure 4. The data are shown in Table S3, the average measured concentrations of diluted CEA serum samples in liver cancer (samples 4-6) and breast cancer (samples 7-9) human serum samples were 33.10 pg/mL and 154.30 pg/mL, respectively. The level of CEA in cancer serum is higher than that in normal serum, the primary normal serum was directly detected (samples 1-3). Then, the known concentrations of CEA are spiked into the serum samples and detected by the same procedure. The recoveries and RSDs were in the ranges of 98.46-101.37% and 1.6-4.6%, respectively. The results

Journal Pre-proof

show acceptable recovery, indicating that the proposed PEC biosensor has great potential for application analysis in clinical samples.

## 4. Conclusions

In summary, a new "on-off-on" biosensor using ZnSe QDs as PEC active material was designed based on 3D DNA nanosphere for CEA detection. The excellent performance of the proposed biosensor results from the high PEC signal of ZnSe QDs and high amplification efficiency of multiple SDA reaction. The photocurrent signal from ZnSe QDs was firstly in "on" state, which was effectively decreased by 3D DNA nanospheres on the electrode to be signal "off" state, then CEA-induced recycling amplification produced numerous S1 to replace DNA nanospheres from electrode, thus the PEC signal became "on" state to achieve sensitive assay of CEA. The present PEC biosensor showed very broad detection range, low detection limit, high sensitivity and well selectivity, and can conveniently detect tumor marker CEA in real serum samples, which has promising potential for the early cancer diagnosis.

## Acknowledgements

This work was supported by the National Natural Science Foundation of China (No. 21575072).

## References

Chen, D. Feng, H. B., Li, J. H., 2012a. Chem. Rev. 112, 6027–6053.

Chen, P., Xiao, T. Y., Li, H. H., Yang, J. J., Wang, Z., Yao, H. B., Yu, S. H., 2012b. ACS Nano. 6, 712−719.

Dai, H., Zhang, S. P., Hong, Z. S., Lin, Y. Y. 2016. Anal. Chem. 88, 9532−9538.

Frens, G., 1973. Nat. Phys. Sci. 241, 20–22.

Gogurla, N., Sinha, A. K., Santra, S., Manna, S.; Ray, S. K., 2014. Sci. Rep. 4, 6483–6491.

Ge, J. J. Zhao, Y., Li, C. L., Jie, G. F., 2019. Anal. Chem. 91, 3546–3554.

Gu, Z.Y., Zou, L., Fang, Z., Zhu, W. H., Zhong, X. H., 2008. Nanotechnology. 19, 135604.

Hariri, A. A., Hamblin, G. D., Gidi, Y., Sleiman, H. F., Cosa, G., 2015. Nat. Chem. 7, 295−300.

Hine, K., Booth, S., Leonard, J., Dykes, P., 1978. Lancet 312, 1337−1340.

Huo, X. L., Yang, H., Zhao, W., Xu, J. J., Chen, H. Y., 2017. ACS Appl. Mater. Interfaces 9, 33360–33367.

Josset, S., Keller, N., Lett, M., Ledoux, M., Keller, V., 2008. Chem. Soc. Rev. 37, 744−755.

Kumar, P., Lambadi, P. R., Navani, N. K., 2015. Biosens. Bioelectron. 72, 340–347.

Journal Pre-proof

Kwon, W., Lee, G., Do, S., Joo, T., Rhee, S., 2014, Small 10, 506−513.

Lee, L. L., Lo, Y. S. 2009. Adv. Funct. Mater. 19, 604–609.

Li, P. P., Cao, Y., Mao, C. J., Jin, B. K., Zhu, J. J., 2019a. Anal. Chem. 91, 1563−1570.

Li, C. L., Li, H. K., Ge, J. J. Jie, G. F., 2019b. Chem. Commun. 55, 3919−3922.

Li, M. T., Meng, G. W., Huang, Q., Zhang, S. L., 2014. Sci. Rep. 4, 4284–4289.

Li, M. J., Zheng, Y. N., Liang, W. B., Yuan, R., Chai, Y. Q., 2017. ACS Appl. Mater. Interfaces 9, 42111–42120.

Li, B. C., Yin, H. S., Zhou, Y. L., Wang, M. H., Wang, J., Ai, S. Y., 2018. Sensors and Actuators B: Chemical. 255, 1744–1752.

Liu, Y. X., Ma, H. M., Zhang, Y., Pang, X. H., Fan, D. W., Wu, D., Wei, Q., 2016. Biosens. Bioelectron. 86, 439–445.

Long, Y. T., Kong, C., Li, D. W., Li, Y., Chowdhury, S., Tian, H., 2011. Small 7, 1624–1628.

Luo, J. S., Karuturi, S. K., Liu, L. J., Su, L. T., Tok, A. L., Fan, H. J., 2012. Sci. Rep. 2, 451−456.

Mayer, K. M., Hafner, J. H., 2011, Chem. Rev. 111, 3828–3857.

Meng, H. M., Liu, H., Kuai, H. L., Peng, R. Z., Mo, L. T., Zhang, X. B., 2016. Chem. Soc. Rev. 45, 2583−2602.

Nishi, H., Kuwabata, S., Torimoto, T. J., 2013. Phys. Chem. C117, 21055−21063.

Ren, K. W., Liu, Y., Wu, J., Zhang, Y., Zhu, J., Yang, M., Ju, H. X., 2016. Nat. Commun. 7, 13580–13589.

Roh, Y. H., Ruiz, R. C., Peng, S., Lee, J. B., Luo, D., 2011. Chem. Soc. Rev. 40, 5730−5744.

Ronkainen, N. J., Halsall, H. B., Heineman, W. R., 2010. Chem. Soc. Rev. 39, 1747–1763.

Shu, J., Qiu, Z. L., Lin, Z. Z., Cai, G. N., Yang, H. H., Tang, D. P., 2016. Anal. Chem. 88, 12539−12546.

Wang, G. L., Xu, J. J., Chen, H. Y., Fu, S. Z., 2009. Biosens. Bioelectron. 25, 791−796.

Wang, L. J., Ren, M., Zhang, Q., Tang, B., Zhang, C. Y., 2017. Anal. Chem. 89, 4488–4494.

Xie, S. J., Zhou, H., Liu, D. Y., Shen, G. L., Yu, R. Q., Wu, Z. S., 2013. Biosens. Bioelectron. 44, 95–100.

Xie, H., Chai, Y., Yuan, Y., Yuan, R., 2017. Chem. Commun. 53, 8368–8371.

Yuan, Y. L., Gan, X. X., Chai, Y. Q., Yuan, R., 2014. Biosens. Bioelectron. 55, 313–317.

Zang, Y., Lei, J. P., Zhang, L., Ju, H. X., 2014. Anal. Chem. 86, 12362−12368.

Journal Pre-proof

Zeng, Y. P., Hu, J., Long, Y., Zhang, C. Y., 2013. Anal. Chem. 85, 6143–6150.

Zhang, Y., Hao, N., Zhou, Z., Hua, R., Qian, J., Liu, Q., Li, H. N., Wang, K., 2017. Chem. Commun. 53, 5810−5813.

Zhang, K. Y., Lv, S. Z., Lu, M. H., Tang, D. P., 2018a. Biosens. Bioelectron. 117, 590–596.

Zhang, P., Jiang, J., Yuan, R., Zhuo, Y., Chai, Y. Q., 2018b. J. Am. Chem. Soc. 140, 9361–9364.

Zhao, Y., Tan, L., Gao, X. S., Jie, G. F., Huang, T. Y. 2018. Biosens. Bioelectron. 110, 239–245.

Zheng, Y. Y., Liang, W. B., Xiong, C.Y., Zhuo, Y., Chai, Y. Q., Yuan, R., 2017. Anal. Chem. 89, 9445−9451.

Zheng, Y. N., Liang, W. B., Xiong, C. Y., Yuan, Y. L., Chai, Y. Q., Yuan, R., 2016. Anal. Chem. 88, 8698–8705.

Zhu, H., Fan, G. C., Abdel-Halim, E. S., Zhang, J. R., Zhu, J. J., 2016. Biosens. Bioelectron. 77, 339–346.

Zimmer, R., Thomas, P. 2001. Cancer Res. 61, 2822−2826.

Journal Pre-proof

Journal Pre-proof

1. A novel 3D DNA nanostructure was assembled by base complementary pairing and RCA reaction.
2. A new “on-off-on” PEC biosensor based on ZnSe QDs and 3D DNA nanosphere was designed for CEA detection.
3. The photocurrent from ZnSe QDs can be effectively reduced by 3D DNA nanospheres for signal “Off” state.
4. The CEA-induced recycling amplification was introduced to achieve sensitive PEC “On” detection of CEA.

Journal Pre-proof

Journal Pre-proof

Xiaoshan Gao,

The first author, original draft

2. Shuyan Niu

The second author, Data curation

3. Junjun Ge

The third author, Formal analysis

4. Qingyu Luan，Validation

5.Guifen Jie

Corresponding author

She is responsible for Writing - review & editing

Xiaoshan Gao, Shuyan Niu, Junjun Ge, Qingyu Luan, Guifen Jie

Sep.9, 2019

Journal Pre-proof

There is no conflict to declare.

Journal Pre-proof

Journal Pre-proof

We declared that we have no conflicts of interest to this work.

Journal Pre-proof